Vibrational Analysis of Trimethylphenyl Ammonium Chloride

Halil Gökce and Semiha Bahçeli

Department of Physics, Faculty of Arts and Science, Süleyman Demirel University, 32260, Isparta, Turkey

Reprint requests to Prof. S. B.; E-mail: bahceli@fef.sdu.edu.tr

Z. Naturforsch. **64a,** 127 – 131 (2009); received March 18, 2008 / revised July 1, 2008

An FT-IR spectrum of trimethylphenyl ammonium chloride (TMPAC) has been recorded in the region 4000 – 400 cm^{-1}. The optimized geometry and vibrational spectrum TMPAC in the ground state have been calculated by using ab initio Hartree-Fock (HF) calculations and the density functional method B3LYP with the 6-31G (d) basis set. The obtained vibrational frequencies and optimized geometric parameters (bond lengths and bond angles) were in very good agreement with the experimental data. The comparison of the observed and calculated results for the vibrational frequencies of TMPAC exhibited that the scaled B3LYP method is superior compared to the scaled HF method. Furthermore the calculated infrared and Raman intensities are also reported.

Key words: Trimethylphenyl Ammonium Chloride; Wavenumbers; IR Spectra; Raman Spectra; HF; DFT.

1. Introduction

Trimethylphenyl ammonium chloride $[(CH_3)_3(C_6H_5)N]Cl$ (TMPAC) has been widely used as methylating agent for morphine in the alkaloid industry for many years [1]. It is also used in agricultural industry [2]. Furthermore, TMPAC in the form of ionic liquids has attracted considerable interest for use as electrolyte in electrochemical cells [3]. Very recently, Stevens and Anderson used the TMPAC as an aromatic compound adsorbed on montmorillonite in an infrared dichroism experiment [4].

In spite of its importance mentioned above, the vibrational assignments of TMPAC are not definitely settled by using ab initio Hartree-Fock (HF) calculation and the density functional theory (DFT/B3LYP) method. It has to be noted that IR and Raman data on TMPAC are not plentiful in literature.

For these reasons the aim of the present study is to determine the vibrational modes and wave numbers of TMPAC in the framework of the DFT/B3LYP and HF methods and to offer the optimized molecular geometry.

2. Experimental and Computational Details

The IR spectrum of TMPAC has been recorded on a Perkin Elmer Spectrum One FT-IR spectrometer at a resolution of 4 cm^{-1} in the transmission mode at room temperature in the region 400 – 4000 cm^{-1}. The computations were performed by using the Gauss-View molecular visualization program and the Gaussian 03 program package on a personal computer [5]. The optimization of the molecular structure of TMPAC in the ground state was verified by the HF and B3LYP calculations with the 6-31G (d) basis set. The sets for HF and B3LYP calculations were scaled with the scaling factors 0.8929 and 0.963, respectively [6].

3. Results and Discussion

The chemical structure and numbering of the atoms of TMPAC are given in Figure 1. Since the chlorine atom of this compound is in an ionized state, it has no influence on both the vibrational and Raman spectra of TMPAC.

The bond lengths and angles of TMPAC optimized by ab initio HF calculations and the DTF/B3LYP method with the 6-31G (d) basis set are listed in Tables 1 and 2, respectively, which also contain experimental results for comparison [7].

The correlation graphics between the calculated and experimental bond lengths and angles of TMPAC are shown in Figs. 2 and 3, respectively. Owing to our calculations the largest difference between the calculated HF bond lengths and experimental values given in Table 1 is about 0.055 Å (Fig. 2). Likewise the biggest difference between the calculated bond angles and ex-

Table 1. Optimized and experimental bond lenghts of TMPAC in the ground state (in Å).

Bond	X-ray [7]	HF	B3LYP
[-3mm] C1-C2	1.41(2)	1.3868	1.3973
C1-C6	1.34(2)	1.3822	1.3925
C1-H7		1.0746	1.0861
C2-C3	1.379(13)	1.3857	1.3962
C2-H8		1.0706	1.0826
C3-C4	1.385(14)	1.3875	1.3959
C3-N12	1.466(14)	1.4949	1.5126
C4-C5	1.37(2)	1.3841	1.3951
C4-H9		1.0776	1.0976
C5-C6	1.33(2)	1.3851	1.3953
C5-H10		1.074	1.0859
C6-H11		1.0747	1.0863
N12-C13	1.508(9)	1.5105	1.5231
N12-C14	1.508(9)	1.5105	1.5231
N12-C15	1.510(13)	1.4871	1.4991

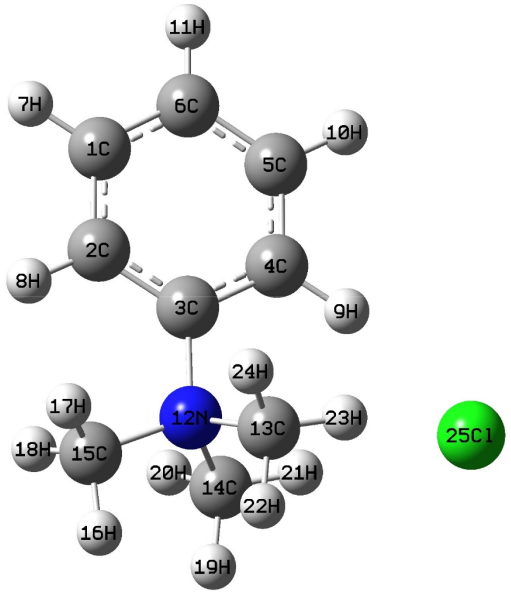

Fig. 1. Chemical structure of TMPAC and numbering of the atoms.

perimental values given in Table 2 is about 1.465° (Fig. 3). In summary the optimized bond lengths and bond angles obtained by HF calculations agree very well with the experimental values.

For the assignment of fundamentals of TMPAC its IR spectrum has been recorded (Fig. 4). TMPAC has the symmetry C_s and contains 25 atoms in the asymmetric unit. The Cartesian displacements of the 25 atoms result in 75 internal modes, i. e. $\Gamma_{\text{inter.}} = 45\text{A}' + 30\text{A}''$, and considering the character table for the C_s point group $\Gamma_{\text{trans.}} = 2\text{A}' + \text{A}''$ and $\Gamma_{\text{rot.}} = \text{A}' + 2\text{A}''$ we find

$$\Gamma_{\text{vib.}} = \Gamma_{75} - \Gamma_{\text{trans.}} = 42\text{A}' + 27\text{A}''$$

Table 2. Optimized and experimental bond angles of TMPAC in the ground state (in °).

Bond	X-ray [7]	HF	B3LYP
C2-C1-C6	120.9(13)	120.416	120.434
C2-C1-H7		119.132	119.076
C6-C1-H7		120.452	120.491
C1-C2-C3	118.6(14)	119.376	119.065
C1-C2-H8		118.174	118.422
C3-C2-H8		122.450	122.513
C2-C3-C4	119.1(11)	120.820	121.35
C2-C3-N12	121.7(9)	121.389	121.091
C4-C3-N12	119.2(10)	117.791	117.559
C3-C4-C5	119.4(12)	118.974	118.592
C3-C4-H9		121.636	121.440
C5-C4-H9		119.389	119.968
C4-C5-C6	122.3(15)	120.835	120.977
C4-C5-H10		118.651	118.523
C6-C5-H10		120.514	120.5
C1-C6-C5	119.7(14)	119.578	119.582
C1-C6-H11		120.143	120.068
C5-C6-H11		120.279	120.35
C3-N12-C13	110.2(5)	109.748	109.513
C3-N12-C14	110.2(5)	109.746	109.513
C3-N12-C15	112.8(9)	112.758	112.470
C13-N12-C14	107.8(7)	109.066	108.872
C13-N12-C15	107.9(6)	107.715	108.2
C14-N12-C15	107.9(6)	107.715	108.2

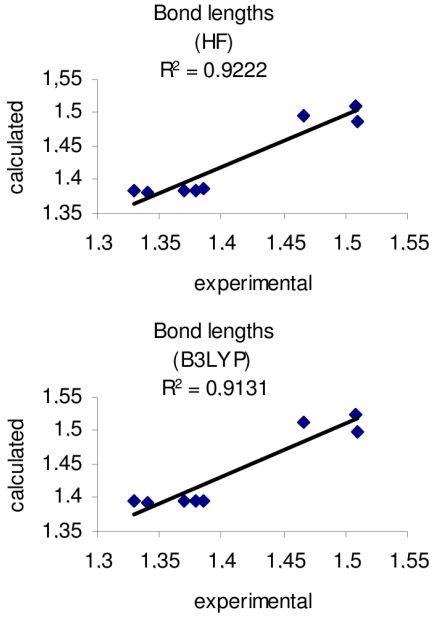

Fig. 2. Correlations between calculated and experimental bond lengths of TMPAC.

vibration modes; here the symmetry A′ denotes the vibration in-plane and the symmetry A″ shows the vibration out-of-plane [8]. All 69 vibrations are active in both the infrared (IR) and Raman (R) spectrum.

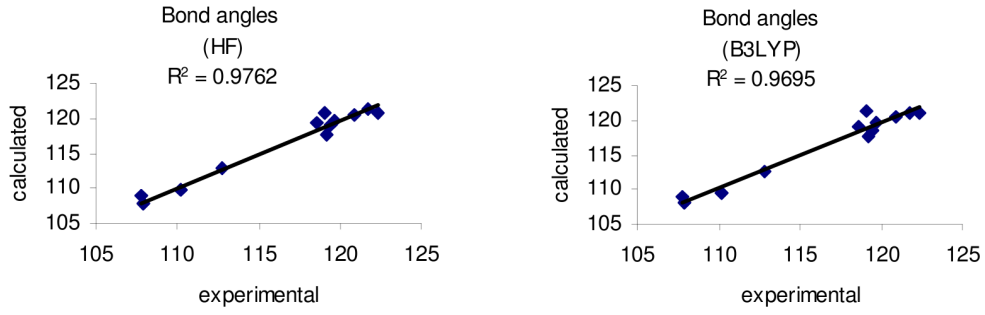

Fig. 3. Correlations between calculated and experimental bond angles of TMPAC.

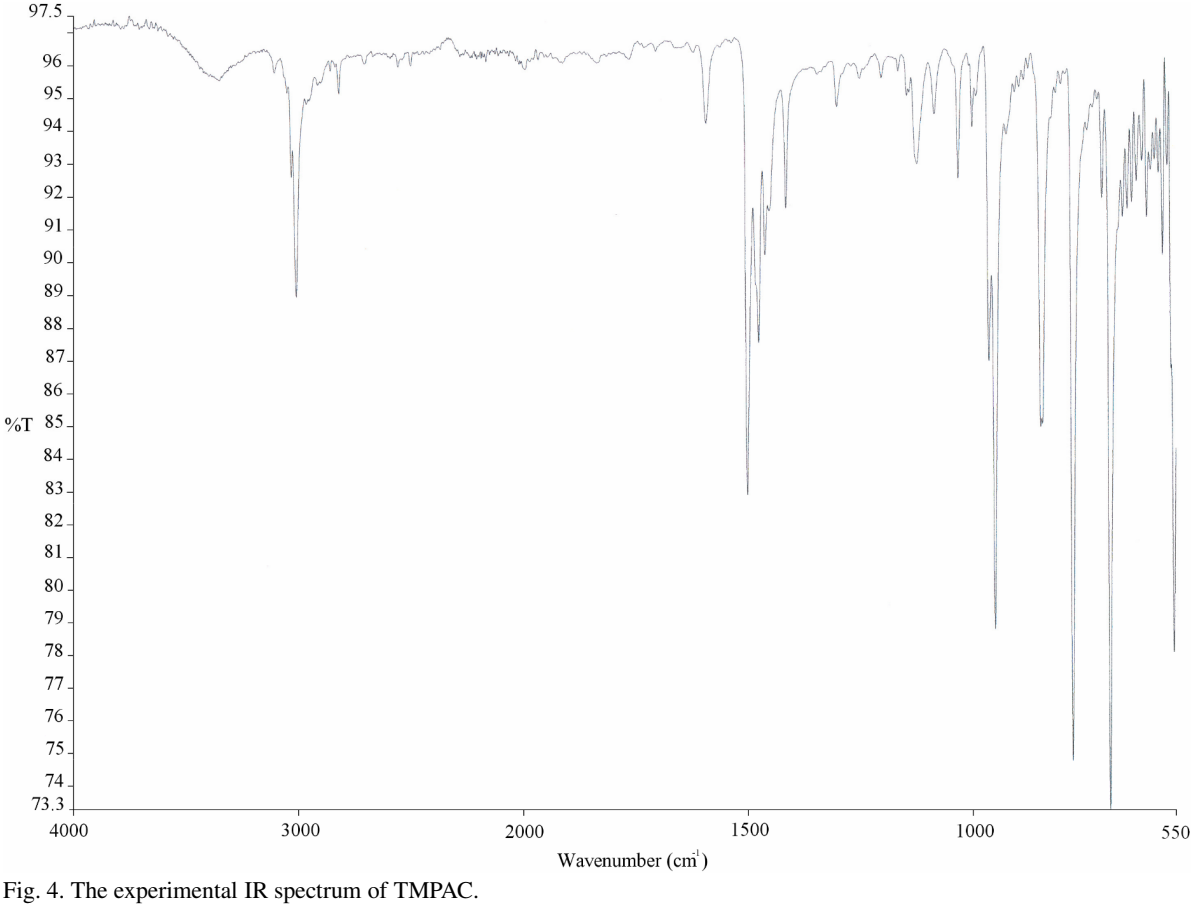

Fig. 4. The experimental IR spectrum of TMPAC.

The assignments of both experimental and calculated IR vibrational frequencies for TMPAC are given in Table 3, where the vibrational frequency modes are numbered from the smallest to the largest frequency values. As seen in Table 3, the experimentally observed peaks in the range 2920 – 3110 cm^{-1} can be assigned to aromatic C-H stretching vibrations [9]. The frequencies calculated by DFT/B3LYP theory using the 6-31G (d) basis set for these vibrational modes exhibit a reliable correspondence in the same wavenumber region. On the other hand, the calculated infrared intensities are usually different when compared with the experimental values for both high- and low-frequency regions. This situation may be evaluated in the framework of the assignment of fundamentals [10]. Due to various reasons, for example, anharmonic effects, the

Table 3. The observed and calculated IR frequencies (cm^{-1}) of TMPAC.

	HF[a]			B3LYP[b]					
Mode	Freq.	IR inten.	Ra inten.	Freq.	IR inten.	Ra inten.	Exp. IR	Exp. Assignment[c]	Assignment[d]
ν_1	55.15	3.2941	4.617	61.65	2.4366	4.3276			op. ring bend. + CH_3 torsion
ν_2	76.62	15.9311	0.5199	92.45	14.9172	0.7118			ip. torsion
ν_3	115.18	7.5471	0.5129	123.19	5.1789	2.9338			CH_3 wag. + CH_2 rock. + ring wag.
ν_4	136.41	0.0014	4.8263	141.44	1.837	2.8405			CH_3 wag. + ring wag.
ν_5	142.81	50.5861	0.1603	167.87	48.6064	0.9425			ip. torsion
ν_6	241.84	0.3854	0.4826	246.52	0.9125	0.5153			CH_3 wag. + ring wag.
ν_7	245.09	0.0404	0.3648	258.04	0.4491	0.5268			CH_3 torsion
ν_8	288.15	5.4845	1.78	297.57	2.193	2.2748			CH_3 torsion
ν_9	331.82	8.3226	2.7461	332.34	1.8894	0.0182			CH_3 rock. + op. ring def.
ν_{10}	333.20	1.6204	0.1107	343.55	9.8239	2.5429			CH_3 torsion + ring torsion
ν_{11}	367.00	4.2105	2.8737	356.74	0.1691	0.1613			CH_3 torsion + op. ring (C-H) bend.
ν_{12}	367.38	0.2678	0.1331	370.16	7.035	3.0291			CH_3 wag. + ring (C-H) str.
ν_{13}	409.11	0.0214	0.3207	406.06	0	0.54			ring wag. + CH_2 rock. + CH_2 wag.
ν_{14}	419.27	0.1501	0.1441	417.00	0.5367	0.1943			CH_3 rock. + op. ring def.
ν_{15}	461.40	0.0466	1.3864	471.55	0.755	1.7634			(N-CH_3) asym. bend. + ring torsion
ν_{16}	545.85	0.8084	5.6842	541.94	12.39	0.7797			ring wag. + CH_3 wag. + CH_2 rock.
ν_{17}	546.79	17.3942	0.4778	548.93	0.5367	5.2053	554 vs	ar. C-H str.	(N-C) str. + ring (C-H) str.
ν_{18}	602.06	1.778	7.0849	605.71	2.8176	7.0913	613 m	ar. C-H str.	ring (C-H) str.
ν_{19}	687.62	1.2076	15.116	685.30	21.1457	2.1271	653 s	op. C-C bend.	op. ring def.
ν_{20}	692.72	32.8607	1.3013	692.50	0.9526	13.363	695 vs	op. C-H bend.	(N-CH_3) sym. str. + (N-C) str. + ring (C-H) str.
ν_{21}	767.19	28.75	1.1345	747.72	22.1033	1.9311	777 vs	op. C-H bend.	op. ring def.
ν_{22}	823.07	37.5239	7.4462	811.74	23.8695	6.1972			(N-CH_3) sym. str. + (N-C) str. + ring (C-H) str.
ν_{23}	862.79	1.501	1.1442	834.67	1.3396	2.4901	847 s	C-H rock.	op. ring (C-H) bend.
ν_{24}	909.31	36.2545	7.0912	890.61	14.1013	3.3494			(N-CH_3) asym. str. + CH_2 twist. + op. ring (C-H) bend.
ν_{25}	954.31	7.3785	0.8816	912.45	6.7913	1.7715			op. ring (C-H) bend. + CH_2 twist.
ν_{26}	963.81	29.7615	7.1825	960.58	21.6104	5.2044	950 vs	op ar. C-H bend.	(N-CH_3) str. + CH_3 rock.
ν_{27}	973.81	2.892	23.3294	961.57	0.4127	0.1089			op. ring (C-H) bend.
ν_{28}	1006.98	0.6524	0.1484	975.69	4.3838	20.2116			ring (CCC) sym. str.
ν_{29}	1011.37	8.4425	19.3178	1021.87	8.3595	23.8249			ip. ring def.
ν_{30}	1060.47	1.6557	2.2161	1035.19	1.2238	3.9566	1032 m	C-N str.	op. ring (C-H) bend.
ν_{31}	1065.11	0.2749	0.476	1057.33	0.0247	1.3866			CH_3 twist. + op. ring (C-H) bend.
ν_{32}	1077.41	0.3853	0.5809	1082.93	1.6793	0.3403			CH_3 rock. + ip. ring (C-H) bend.
ν_{33}	1082.25	6.567	0.7096	1091.18	6.0242	4.4563			ip. ring (C-H) bend. + (N-C) str. + CH_3 rock.
ν_{34}	1101.92	11.6463	4.329	1117.18	0.0778	1.1067			CH_3 rock.
ν_{35}	1126.67	1.3697	1.858	1117.70	1.4929	10.0074	1126 m	C-N str.	CH_3 rock. + CH_2 twist. + ip. ring (C-H) bend.
ν_{36}	1126.70	3.8906	6.5928	1158.36	0.1054	3.2858			ip. ring (C-H) bend.
ν_{37}	1191.08	0.904	2.4937	1198.96	1.8739	2.4005			ip. ring (C-H) bend.
ν_{38}	1200.46	1.2639	0.343	1221.50	0.6161	0.7915			(N-CH_3) asym. str.
ν_{39}	1242.53	13.3523	1.4514	1224.38	3.9175	0.4948			(N-CH_3) asym. str.
ν_{40}	1251.19	11.4685	1.4961	1262.83	1.0336	7.9824	1251 m	C-N str.	CH_3 rock. + (N-C) str.
ν_{41}	1287.14	6.4664	3.1695	1310.47	3.7063	0.081	1301 m	C-N str.	ip. ring (CCC) asym. str. + CH_2 wag.
ν_{42}	1351.06	0.6307	2.435	1344.34	0.1836	3.2395	1341 bw	C-N str.	ip. ring (C-H) bend.
ν_{43}	1422.00	0.1351	5.9923	1408.41	0.1672	7.0287			CH_3 sym. bend.
ν_{44}	1428.76	3.6317	4.9842	1416.73	11.0687	5.0927	1416 m	CH_3 sym. bend.	CH_3 sym. bend.
ν_{45}	1443.37	4.0067	18.3306	1434.61	3.7768	19.9568			CH_3 sciss.
ν_{46}	1448.23	11.0807	2.9543	1444.06	10.247	2.3477			CH_2 bend. + CH_3 sciss. + ip. ring (C-H) bend.
ν_{47}	1462.78	1.0599	0.7668	1454.02	5.5316	4.4028			CH_3 sym. bend. + ip. ring (C-H) bend.
ν_{48}	1463.15	0.3008	13.326	1464.93	0.4506	18.0087	1461 s	CH_3 asym. bend.	CH_3 twist.
ν_{49}	1471.70	33.7506	18.9726	1468.90	24.3854	11.4138			CH_3 asym. bend. + ip. ring (C-H) bend.
ν_{50}	1483.61	4.1176	9.6284	1481.95	3.1934	12.6248	1477 s	CH_3 asym. bend.	CH_3 sciss. + ip. ring (C-H)
ν_{51}	1486.87	23.2645	7.1463	1488.60	18.9437	3.5726			CH_3 twist. + CH_3 asym. bend.
ν_{52}	1498.32	77.8298	3.677	1493.67	65.1876	3.2854			ip. ring (C-H) + CH_3 asym. bend.
ν_{53}	1502.58	23.9695	2.0456	1502.19	16.0171	2.7559	1501 vs	CH_3 asym. bend.	CH_3 sciss. + ip. ring (C-H) bend.
ν_{54}	1602.09	2.3425	13.934	1591.33	0.6836	14.6472			ring (CCC) asym. str.
ν_{55}	1610.06	6.9745	11.5802	1592.48	5.7457	10.8944	1593 m	ar. C-C str.	ring (CCC) asym. str.
ν_{56}	2892.62	32.7353	14.9885	2864.20	63.0897	48.5548			CH_3 sym. str.
ν_{57}	2897.34	58.7284	154.158	2873.70	151.106	154.57			CH_3 sym. str. + ring (C-H) str.
ν_{58}	2920.21	22.2702	125.152	2919.77	621.18	473.306	2920 w		CH_3 sym. str. + ring (C-H) str.
ν_{59}	2970.70	99.7891	191.45	2985.15	15.2231	88.7373	2963 w	CH asym. str.	CH_3 sym. str.
ν_{60}	2987.16	3.3564	16.8048	3014.54	0.3067	1.8039	3007 s	CH asym. str.	CH_3 asym. str.
ν_{61}	2991.02	52.547	45.5538	3021.84	88.4597	146.567	3029 w	ar. CH str.	CH_3 asym. str.
ν_{62}	2998.18	0.8265	5.562	3065.13	3.0689	24.2407	3048 w	ar. CH str.	CH_2 asym. str.
ν_{63}	3004.62	92.0422	132.944	3065.83	7.1408	32.9198			CH_3 asym. str. + CH_2 asym. str.
ν_{64}	3006.66	88.1443	98.4936	3076.10	15.6854	130.48			CH_3 asym. str. + CH_2 asym. str. + ring (C-H) asym. str.
ν_{65}	3007.56	8.4892	40.2393	3077.26	5.3506	40.6295			CH_2 asym. str.
ν_{66}	3011.25	8.0881	71.5544	3077.58	2.9977	36.1892			ring (C-H) asym. str. + CH_3 asym. str.
ν_{67}	3025.02	8.2591	94.2001	3089.70	7.483	94.2116			ring (C-H) asym. str.
ν_{68}	3036.93	16.4175	172.461	3099.79	16.3883	197.24	3104 w	ar. CH str.	ring (C-H) asym. str.
ν_{69}	3060.41	6.5149	88.196	3120.45	6.6886	113.43			ring (C-H) sym. str.

[a] Scaling factor = 0.8929. [b] Scaling factor = 0.963. [c] Taken from [9]. [d] On the basis of DFT calculation: ip., in-plane; op., out-of-plane; bend., bending; rock., rocking; sciss., scissoring; str., stretching; wag., wagging; sym., symmetric; def., deformation; asym., asymmetric; twist., twisting.

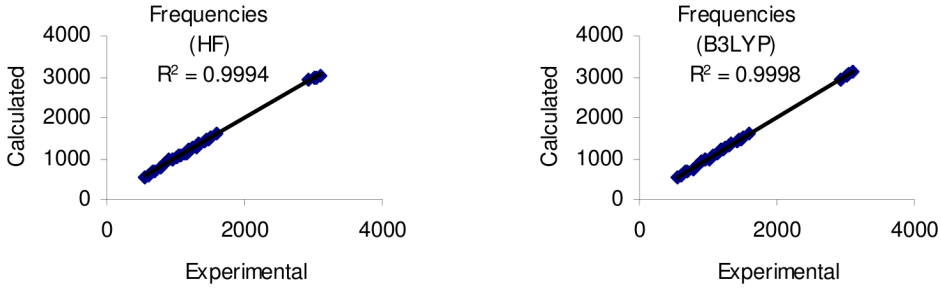

Fig. 5. Correlations between calculated and experimental molecular vibrational frequencies of TMPAC.

vibrational intensities could not be considerably identified by infrared and Raman spectroscopy. Therefore, we payed attention to the frequency only.

Considering Table 3, it can be easily stated that the experimental and theoretical vibration values are in a good agreement with each other. The correlations between them are shown in Figure 5. The correlation values for HF and B3LYP are 0.8929 and 0.963, respectively. The correlation values in Fig. 5 show that the results of DFT/B3LYP calculations are more likely than ab initio HF calculation for vibrations.

4. Conclusion

As a conclusion, the results calculated by the DFT/B3LYP method give better fits to experimental ones than those calculated by the HF method. The excellent agreement between the frequencies calculated by B3LYP with the 6-31G (d) basis set and the ones found in the experiment exhibit that the density functional theory is more suitable for providing information about vibrational spectra of the mentioned compound. On the other hand, ab initio HF methods are the more suitable approach to optimize bond lengths and angles.

Acknowledgements

This study was supported by the Unit of Management of Scientific Research Projects within the Project No. 984-m-05 of Süleyman Demirel University, Isparta, Turkey.

[1] C. K. Ingold and C. S. Patel, J. Chem. Soc. **1**, 69 (1933).
[2] G. P. Rizzi, J. Agric. Food **38**, 1941 (1990).
[3] J. Tiang, M. J. Chollier Brym, G. Dube, A. Lasia, and G. M. Brisard, Surf. Coat. Technol. **201**, 10 (2006).
[4] J. J. Stevens and S. J. Anderson, Clays Clay Miner. **44**, 132 (1996).
[5] M. J. Frisch, G. W. Trucks, H. B. Schlegel, G. E. Scuseria, M. A. Robb, J. R. Cheeseman, J. A. Montgomery, Jr., T. Vreven, K. N. Kudin, J. C. Burant, J. M. Millam, S. S. Iyengar, J. Tomasi, V. Barone, B. Mennucci, M. Cossi, G. Scalmani, N. Rega, G. A. Petersson, H. Nakatsuji, M. Hada, M. Ehara, K. Toyota, R. Fukuda, J. Hasegawa, M. Ishida, T. Nakajima, Y. Honda, O. Kitao, H. Nakai, M. Klene, X. Li, J. E. Knox, H. P. Hratchian, J. B. Cross, V. Bakken, C. Adamo, J. Jaramillo, R. Gomperts, R. E. Stratmann, O. Yazyev, A. J. Austin, R. Cammi, C. Pomelli, J. W. Ochterski, P. Y. Ayala, K. Morokuma, G. A. Voth, P. Salvador, J. J. Dannenberg, V. G. Zakrzewski, S. Dapprich, A. D. Daniels, M. C. Strain, O. Farkas, D. K. Malick, A. D. Rabuck, K. Raghavachari, J. B. Foresman, J. V. Ortiz, Q. Cui, A. G. Baboul, S. Clifford, J. Cioslowski, B. B. Stefanov, G. Liu, A. Liashenko, P. Piskorz, I. Komaromi, R. L. Martin, D. J. Fox, T. Keith, M. A. Al-Laham, C. Y. Peng, A. Nanayakkara, M. Challacombe, P. M. W. Gill, B. Johnson, W. Chen, M. W. Wong, C. Gonzalez, and J. A. Pople, Gaussian 03, Revision C.02, Gaussian, Inc., Wallingford CT 2004.
[6] J. B. Foresman and A. Frish, Exploring Chemistry with Electronic Structure Methods, 2nd ed., Gaussian, Inc., Pittsburgh, PA 1996.
[7] P. Nockemann and G. Meyer, Acta Cryst. E **58**, m527 (2002).
[8] D. M. Bishop, Group Theory and Chemistry, Clarendon Press, Oxford 1973.
[9] R. M. Silverstein and F. X. Webster, Spectroscopic Identification of Organic Compounds, 6th ed., John Willey & Sons, New York 1998.
[10] J. E. del Bene, J. Am. Chem. Soc. **101**, 6184 (1979).